Adsorbate-induced demagnetization and restructuring of ultrathin magnetic films: CO chemisorbed on γ-Fe/Cu(100)

D. Spišák and J. Hafner
Institut für Materialphysik and Center for Computational Materials Science, Universität Wien, Sensengasse 8, A-1090 Wien, Austria
(Received 21 December 2000; published 8 August 2001)

First-principles local-spin-density (LSD) investigations of the structural, magnetic, and electronic properties of clean and CO-adsorbed ultrathin γ-iron films epitaxially grown on Cu(100) surfaces demonstrate that both the geometrical and the magnetic structures of the films are profoundly modified by the adsorption of CO. The enhanced magnetic moments of the top-layer atoms are strongly quenched by the presence of the adsorbate. Due to the pronounced magnetovolume effect, this leads also to a correlated change in the interlayer relaxations. Strikingly, the adsorbate-induced demagnetization is primarily limited to those surface atoms directly bonded to the adsorbate. This leads to the formation of an in-plane magnetic pattern in a partially adsorbate-covered film. The comparison of the calculated vibrational eigenfrequencies of the CO adsorbate with experiment confirms the picture based on the LSD calculations.

DOI: 10.1103/PhysRevB.64.094418 PACS number(s): 75.70.−i, 68.43.Bc, 71.15.Mb

I. INTRODUCTION

The physical properties of magnetic systems with reduced dimensions (ultrathin films, clusters, nanowires) have been studied extensively during the last years, motivated by their large potential in magnetic and magneto-optic storage technologies and by fundamental interest in the structure-property relationship. The design of tailor-made magnetic structures at surfaces and in ultrathin films is considered to be of central importance for the development of future devices. A particularly difficult problem in the center of technological efforts is to generate microscopic magnetic patterns on surfaces or in ultrathin layers. It is now well established that atomic or molecular adsorbates can eventually demagnetize magnetic surface layers,[1] but only very recently it was pointed out[2] that the adsorbate-induced demagnetization is strictly localized, being limited to those surface atoms directly bonded to the adsorbate. However, it remains largely unknown whether such localized changes in the magnetism are important in determining atomic geometries and stabilities.

In the present paper we report on investigations of CO adsorption on ultrathin films of γ-iron epitaxially grown on Cu(100) substrates. Fe/Cu(100) films have attracted considerable attention as a model system for studying the correlation between atomic structure and magnetism. The particularly interesting properties of this system are caused by the fact that at the density of the Fe films stabilized by epitaxial growth ferromagnetic high and low moment states, antiferromagnetic and nonmagnetic states differ only very little in energy and hence the magnetic ground state of Fe/Cu(100) will depend critically on volume and symmetry. Indeed, a vast experimental[3–16] and theoretical effort[17–22] was needed to converge towards a consistent picture. For room-temperature grown films for which a layer-by-layer growth has been reported, the following structural and magnetic phase diagram has been widely accepted: (a) Films with up to about $3-4$ monolayers (ML) are ferromagnetic (FM) throughout the film; the atomic structure is tetragonally distorted face-centered cubic (fcc) with an expanded volume and a considerable three-dimensional (3D) lattice modulation (regime I). (b) In the regime between $4-5$ and about 11 ML, the bulk of the film has been characterized as an undistorted antiferromagnetic (AFM) fcc Fe with a density close to that of bulk γ-Fe and a small net magnetic moment. The net magnetic moment is attributed to the FM coupling between the surface and first subsurface layer, whose interlayer distance is tetragonally expanded. In this regime a bilayer AFM sequence ($\uparrow\uparrow\downarrow\downarrow\cdots$) is found in films with an even number of monolayers; in films with an odd number of layers various antiferromagnetic structures are energetically nearly degenerate (regime II). At a thickness of four monolayers, the two magnetic phases coexist at low temperatures.[13–15] Upon heating, a gradual transformation to phase II occurs. (c) In films with more than 11 ML the fcc structure becomes unstable and transforms to a body-centered cubic (bcc) structure and the films are ferromagnetic. Although experiment and theory agree on the same general picture, certain quantitative differences between the structural predictions and low-energy electron-diffraction (LEED) analyses, concerning in particular the distance between the top layers, exist. Local-spin-density calculations tend to predict a modest inward relaxation of the top layer (i.e., the expansion caused by the increased magnetic moments of the surface atoms is compensated or even overcompensated by the contraction coming from the increased bond order of the back bonds to the deeper layers), whereas LEED studies show no or even a slight outward relaxation.

For Fe films grown at low temperatures, where layer-by-layer growth cannot be realized, very different structural and magnetic properties have been reported. The tetragonally expanded ferromagnetic phase is stabilized for up to five monolayers. Above that thickness the Fe film directly transforms to the bcc structure without passing through the intermediate isotropically fcc phase.[16]

Very recently it has been shown that hydrogen adsorption stabilizes the tetragonally expanded phase of room-temperature grown films for up to four monolayers, while the

phase boundary of the antiferromagnetic fcc films and the ferromagnetic bcc films is shifted from about 10–11 down to 8 monolayers.[23] The transition between regimes I and II in a four-monolayer film is reversible upon hydrogen adsorption and desorption. Only slight enhancement of the surface magnetization upon hydrogen adsorption was reported.[23,24] A possible scenario explaining these observations is that hydrogen is adsorbed in, and not on top of, the Fe film, leading to a volume expansion stabilizing the ferromagnetic phase.

The dissociation of CO on iron surfaces has been widely investigated due to its relevance for the Fischer-Tropsch synthesis.[25,26] The investigation of the adsorption of carbon monoxide on thin γ-Fe films grown on Cu(100) has led to results that are surprising in many respects. On α-Fe surfaces CO adsorbed dissociates at temperatures of about 300 K; on γ-Fe/Cu(100) films only molecular desorption at higher temperatures was observed.[27–29] Whereas for CO on α-Fe a tilted or ''side-on'' configuration has been reported; on γ-Fe surfaces CO adsorbs in an upright position.[28] The preferred adsorption site is the bridge position at low coverage, at higher CO uptakes, occupation of the on-top sites has been reported.[29] Recently, it has also been observed that the presence of CO during the growth of Fe films on Cu(100) has a stabilizing influence on the γ-phase,[30] and films with up to 60 monolayers retain the fcc structure. This stabilizing influence has been attributed to a collaborative surfactant effect of carbon and oxygen and to the incorporation of carbon into the growing fcc lattice. Nevertheless, although the strong interaction of adsorbed CO with the thin Fe films is evident, very little is known about the changes in the surface structure and of the magnetic properties induced by CO adsorption.

The present work reports *ab initio* density-functional studies of the adsorption of CO on four-monolayer films of Fe grown on Cu(100). This film thickness corresponds to the transition regime from ferromagnetic, tetragonally expanded films to antiferromagnetic films with an isotropic fcc structure. For low-temperature grown films an irreversible structural and magnetic phase transition has been reported. It can therefore be expected that such films are particularly sensitive to adsorbate-induced changes in their surface properties. For films with various magnetic configurations, the stable adsorption geometries have been determined for CO coverage of 0.5 and 1 monolayers. The adsorbate-induced changes in the interlayer relaxations and in the magnetic moments have been determined. For the ground-state solutions the vibrational eigenfrequencies of adsorbate have been obtained by diagonalization of a dynamical matrix constructed from the appropriate interatomic forces.

II. METHODOLOGY

Our calculations have been performed using a spin-polarized version of the Vienna *ab initio* simulation program VASP.[31–34] VASP performs an iterative solution of the Kohn-Sham equations of local-spin-density-functional theory via a minimization of the norm of the residual vector to each eigenstate and optimized charge- and spin-density mixing routine. Electronic eigenstates are expanded in terms of plane waves within the projector-augmented-wave (PAW) formalism.[34,35] The PAW method is an all-electron band-structure technique. It is very closely related to the ultrasoft pseudopotential method.[36,37] The PAW approach shares the computational efficiency of the pseudopotential technique, but as an all-electron technique it allows to avoid the problems related to the linearization of the core-valence exchange interaction. This advantage is particularly valuable in treating magnetic 3*d* transition metals. Within the PAW approach it is possible to restrict the basis set to plane waves with a maximum kinetic energy of 300 eV. For any details concerning the construction of the PAW potentials we refer to the previous works.[34,35] VASP allows to calculate the Hellmann-Feynman forces acting on the atoms, hence a full structural optimization of the adsorbate/film/substrate system may be performed very efficiently using a quasi-Newton technique.

In our calculations we used the exchange-correlation functional based on the quantum Monte Carlo calculations of Ceperley and Alder as parametrized by Perdew and Zunger,[38] using the spin interpolation according to Vosko *et al.*[39] and adding generalized gradient corrections (GGC's) in the form proposed by Perdew *et al.*[40,41] The use of generalized gradient corrections is essential for a correct prediction of the ground-state properties of iron: without GGC's, bulk Fe is predicted to be hexagonal and nonmagnetic; with GGC's the correct ferromagnetic bcc ground state is found. In addition, magnetovolume effects are much better described in a generalized gradient approximation. This is particularly important for a study of the structural and magnetic transition between regimes I and II of Fe films grown on Cu(100).[20,21]

The Fe/Cu(100) system has been modeled by a periodically repeated slab with four Fe layers and four layers of Cu representing the substrate. For a coverage of 0.5 ML of CO a (2×1) surface cell has been used; calculations at a full coverage have been performed using a (1×1) surface cell. In all calculations the lateral lattice constant has been fixed at the equilibrium value calculated for Cu using GGC's [$a_{\mathrm{Cu}_{(\mathrm{theor})}}=3.637$ Å, $a_{\mathrm{Cu}_{(\mathrm{expt})}}=3.61$ Å]. All interlayer distances within the Fe film, at the interface and the distance between the two top layers of the substrate, have been allowed to relax; the atomic positions in the deeper layers of the substrate have been kept fixed. CO molecules have been placed into on-top, bridge, and hcp hollow positions, with the molecular axis perpendicular to the surface. The distances between the top Fe layer and the C atom and the C–O bond length have been optimized. At a coverage of only half a monolayer of CO, a corrugation of the entire Fe film and of the uppermost part of the substrate was admitted. Brillouin-zone integrations have been performed using a set of Monkhorst-Pack[42] special *k* points and a modest Gaussian smearing of $\sigma=0.2$ eV. For the (1×1) surface cell of the fully CO-covered films, a $(11\times11\times1)$ grid corresponding to 21 *k* points was used for calculating the structural relaxation of the films. For the final calculation of the total energy, the magnetic moments, and the electronic structure, the grid was refined to $(15\times15\times1)$. For the (2×1) surface cell used at a coverage of $\theta=0.5$ ML, *k*-point meshes of $(12\times6\times1)$ and $(16\times8\times1)$ corresponding to 18 and 32 *k* points, respec-

TABLE I. Structural and magnetic properties of clean and CO-covered ($\theta=1$ ML) γ-Fe/Cu(100) films as calculated for different magnetic configurations of the 4-ML film. The energy difference ΔE (in meV/cell) is quoted with respect to the stable configuration of the clean (uudd) and the CO-covered (uuud) film. Δd_{ij} stands for the change of the interlayer distance with respect to the calculated Cu interlayer distance (in %), μ_i for the local magnetic moment (in μ_B) in each layer. $\Sigma\Delta d_{ij}$ stands for the relative change in the total film thickness, $\Sigma\mu_i$ for the total magnetic moment of the film.

Magnetic configuration	Adsorption site	ΔE	$\Delta d_{\text{Cu-Cu}}$	$\Delta d_{\text{Cu-Fe}}$	μ_4	Δd_{43}	μ_3	Δd_{32}	μ_2	Δd_{21}	μ_1	$\Sigma\Delta d_{ij}$	$\Sigma\mu_i$
uudd	clean	0			2.62		2.18		−2.20		−2.82		−0.22
			1.0	2.0		2.6		−4.9		0.6		−1.7	
	bridge	104			2.63		2.12		−1.48		−2.18		1.09
			1.6	2.5		2.4		−8.2		−5.6		−11.4	
	hollow	125			2.63		2.25		−1.98		−1.23		1.67
			1.2	2.2		3.3		−5.0		−2.5		−4.2	
	top	244			2.58		2.19		−1.06		−0.44		3.27
			0.6	1.8		1.3		−4.6		−14.5		−17.8	
uuuu	clean	49			2.63		2.61		2.61		2.84		10.69
			1.0	1.9		2.9		3.8		−0.4		6.3	
	bridge	207			2.62		2.58		2.50		1.56		9.26
			1.7	2.6		3.3		1.8		1.7		6.8	
	hollow	169			2.63		2.59		2.51		1.32		9.03
			1.1	2.2		2.4		1.0		−2.5		0.9	
	top	390			2.62		2.58		2.41		1.48		9.09
			0.7	2.3		2.6		2.0		14.1		18.7	
uuud	clean	221			2.61		2.54		1.91		−2.23		4.84
			1.1	2.3		3.5		3.1		−6.9		−0.3	
	bridge	0			2.63		2.57		1.81		−0.89		6.12
			1.0	2.1		3.3		0.9		−12.4		−8.2	
	hollow	119			2.63		2.57		2.39		−0.54		7.05
			1.3	2.3		4.1		2.5		0.9		7.5	
	top	391			2.63		2.60		1.69		−0.87		6.05
			0.9	2.0		3.6		2.1		−15.2		−9.5	

tively, have been used. In all cases full convergence could be achieved.

For the clean 4-ML Fe/Cu(100) films calculations predict a bilayer antiferromagnetic ordering (we use the notation uudd with the meaning u=up, d= down for the orientation of the magnetic moments in the four Fe layers, starting with the Fe layer at the interface and ending at the free surface of the film) in the ground state, with only small magnetic energy differences between the ground state and ferromagnetic uuuu configuration and a slightly larger magnetic energy difference for a partially antiferromagnetic uuud configuration.[21,22] For these three configurations, CO adsorption has been studied in detail. For the most stable magnetic configurations of the substrate, the vibrational eigenfrequencies of the adsorbate have been calculated using the direct method, i.e., the force constants for the stretching and frustrated translation modes have been calculated and the dynamical matrix has been diagonalized.

III. RESULTS

Our results for the atomic geometries, magnetic moments, magnetic energy differences of the Fe films, the adsorption energies, and geometries are compiled in Tables I–IV where we summarize for comparison also the properties of the clean films. In the ferromagnetic uuuu configuration, all magnetic moments are enhanced over the theoretical magnetic moment of bulk γ-Fe ($\mu=2.35\mu_B$), varying between about $2.6\mu_B$ in the interior of the film and $2.84\mu_B$ at the free surface. All interlayer distances in the Fe film except between the top layers are expanded due to the larger volume of ferromagnetic Fe, leading to the experimentally observed tetragonal distortion characteristic of regime I. At the free surface, the magnetovolume effect is counterbalanced by the surface contraction typical for transition-metal surfaces. In the bilayer AFM configuration, surface and interface moments are essentially the same as in the FM phase, but the moments in the interior of the film where the direction of the spins changes are only about $2.2\mu_B$. Distances between ferromagnetically coupled layers are expanded, and those between antiferromagnetically coupled layers are contracted (again with the exception of the distance between the top layers) so that on average the structure is isotropically fcc. In the mixed magnetic configuration uuud with an antiferromagnetic coupling only between the top layers, the frustration leads to a reduction of the moments in the antiferromag-

TABLE II. Adsorption properties of CO on γ-Fe/Cu(100) films (monolayer coverage): Adsorption energies E_{ad} (in eV/molecule), height z_C of the C atom above the top layer of the film (in Å), bond length $d_{C\text{-}O}$ of the molecule (in Å), adsorption-induced change of the film thickness Δd (in % of the calculated interlayer distance in fcc Cu), and adsorption-induced change $\Delta\mu$ of the magnetization of the film (in μ_B).

Magnetic configuration	Adsorption site	E_{ad}[a]	E_{ad}[b]	z_C	$d_{C\text{-}O}$	Δd	$\Delta\mu$
uudd	bridge	−1.074	−1.074	1.49	1.17	−9.7	1.31
	hollow	−1.053	−1.053	0.95	1.20	−2.5	1.89
	top	−0.934	−0.934	1.49	1.16	−16.1	3.49
uuuu	bridge	−0.971	−1.019	1.48	1.17	0.5	−1.43
	hollow	−1.009	−1.057	0.96	1.20	−5.4	−1.64
	top	−0.788	−0.836	1.58	1.16	12.4	−1.60
uuud	bridge	−1.178	−1.399	1.51	1.17	−7.9	1.28
	hollow	−0.787	−1.008	0.94	1.21	7.8	2.21
	top	−1.059	−1.281	1.80	1.16	−9.2	1.21

[a]The adsorption energy is calculated with respect to the same magnetic configuration of the clean films.
[b]The adsorption energy is calculated with respect to the magnetic ground state (uudd) of the clean film.

netic upper half of the film; again expansion and contraction of the interlayer distances approximately compensate such that the structure is fcc on average. The magnetic energy difference relative to the uudd ground state per cell is 49 meV for the ferromagnetic phase and 221 meV/cell for the uuud configuration. In the following we investigate the changes induced by the adsorption of CO. We begin by discussing the somewhat simpler case of a film covered by a compact monolayer of CO.

A. Fe/Cu(100) covered by a monolayer of CO

1. Structure and magnetism

As the possible location of the adsorbed CO molecule, the symmetric on-top, bridge, and hollow positions have been examined. The molecule has been placed in an upright position, with the C atom pointing towards the surface. The relaxation process allowed for a canting of the adsorbate, but in all cases the vertical orientation remained unchanged.

For a ferromagnetic film, the fourfold hollow is the stable adsorption site (see Table I). The adsorption leads to a strong reduction of the magnetic moments in the surface layer and to a slight reduction of the moments in the second layer. The magnetism of the deeper layers remains unaffected by the adsorption. Altogether the magnetization of the film is reduced by $1.6\mu_B$. The decrease of the magnetic moments leads to a reduced magnetovolume effect such that the CO-covered film is fcc on average. Adsorption in the bridge site has a weaker effect on the magnetism of the film. In this case, the reduced magnetovolume effect is compensated by a weak adsorbate-induced outward relaxation of the top layer, so that on average the film structure is not affected by the adsorption. Adsorption in the energetically less favorable top position (the difference in the adsorption energies is 221 meV/cell, see Table II) leads to a reduction of the magnetization comparable to that for adsorption in the hollow position and to a surprisingly large outward relaxation of the top layer indicating a back donation of electrons from the adsorbate to antibonding states of the substrate atoms, weakening the bonds between the top layer and the bulk of the film. This shows that the details of the adsorbate-substrate bonding are rather sensitive to the adsorption geometry.

For the bilayer antiferromagnetic (uudd) configuration, which is stable for the clean film, adsorption in the bridge position is energetically favored. In this case, a large reduction of the magnetic moment is calculated not only for the top layer (from $2.82\mu_B$ to $2.18\mu_B$), a larger decrease is found in the second layer (from $2.20\mu_B$ to $1.48\mu_B$), and even the moment in the third layer is slightly reduced (see Table I). The decrease of the magnetic moments is accompanied by a reduction of the interlayer spacings between the first three layers such that the thickness of the Fe film is reduced by 11.4% with respect to the calculated Cu interlayer distance. For the clean film, the large negative moments in the top bilayer outweigh the smaller positive moments in the second bilayer, such that the total magnetization of the film is negative, although quite small. The reduction of the moments in the top layers due to chemisorption of CO leads to a reversal of the sign of the magnetization and to an increase of its amplitude. Adsorption in a fourfold hollow leads to an adsorption energy which is lower only by 21 meV/cell. In this case, the reduction of the surface moment is even larger (from $2.82\mu_B$ to $1.23\mu_B$), but the effect is more confined to the surface. Adsorption-induced changes in the interlayer distances are also restricted to the top bilayer, where the reduced magnetovolume effect is found to outweigh the adsorption-induced outward relaxation. Adsorption in a top site is predicted to have a dramatic influence on both magnetism and structure of the film (see Table I), but is energetically disfavored by a rather large amount. In these two cases, adsorption leads again to the formation of a raised positive total magnetization.

In the mixed magnetic uuud phase adsorption in the bridge site is again favored. The uuud configuration was cho-

TABLE III. Structural and magnetic properties of clean and CO-covered ($\theta = 0.5$ ML) γ-Fe/Cu(100) films as calculated for different magnetic configurations of the film. The energy difference ΔE (in meV/cell) is quoted with respect to the stable configuration of the clean (uudd) and the CO-covered (uudd) film. Δd_{ij} stands for the change of the interlayer distance with respect to the ideal Cu lattice (in %), μ_i for the local magnetic moment (in μ_B) in each layer. $\Sigma \Delta d_{ij}$ stands for the relative change in the total film thickness, $\Sigma \mu_i$ for the total magnetic moment of the film.

Magnetic configuration	Adsorption site	ΔE	Δd_{32}	μ_2	Δd_{21}	μ_1	$\Sigma \Delta d_{ij}$	$\Sigma \mu_i$
uudd	clean	0		−2.20		−2.82		−0.22
			−4.9		0.6		−1.7	
	bridge	0		−2.02		−1.40		0.62
				−2.02		−2.88		
			−6.3		0.4		−3.2	
			−6.3		0.3			
	hollow	54		−1.94		−2.22		0.65
				−2.01		−2.22		
	top	198		−1.96		−1.34		0.70
				−1.96		−2.92		
uuuu	clean	98		2.61		2.84		10.69
			3.8		−0.4		6.3	
	bridge	93		2.54		1.51		9.96
				2.54		2.92		
			2.7		3.2		7.1	
			2.7		0.3			
	hollow	161		2.61		2.29		10.06
				2.51		2.29		
	top	362		2.35		0.52		9.27
				2.35		2.91		
uuud	clean	442		1.92		−2.23		4.84
			3.1		−6.9		−0.3	
	bridge	89		2.10		−0.55		5.74
				2.10		−2.55		
			1.9		−9.0		−3.4	
			1.9		−7.8			
	hollow	372		2.19		−1.97		5.30
				1.93		−1.97		
	top	231		2.04		−0.76		5.60
				2.04		−2.53		

sen with the intention of examining the possibility that the adsorbate-induced demagnetization of the surface layer eventually breaks the strong ferromagnetic coupling of the surface bilayer. The negative magnetic moment in the Fe top layer is strongly quenched (from $-2.23\mu_B$ to $-0.89\mu_B$) and the moment in the second layer is somewhat reduced as well (see Table I). The overall magnetization of the film is enhanced due to the reduction of the antiferromagnetic component. The reduction of the subsurface moment μ_2 also leads to a contraction of the interlayer spacing between the second and third layers. A much stronger relaxation, however, occurs between the two topmost layers where the inward relaxation is now nearly twice as large as for the clean film—evidently this can be related neither to a magnetovolume effect nor to a simple back-donation effect. We shall come back to this point below. Adsorption in the on-top position leads to similar magnetic and structural effects, but is energetically unfavorable. Adsorption in the fourfold hollow leads to an even stronger quenching of the antiferromagnetic surface moment, but to an enhanced magnetization of the second layer. The nearly ferromagnetic character of the film leads to an expansion of the interlayer distances. Altogether we find a very complex pattern of adsorbate-induced changes in the magnetization and in the relaxation properties of the films.

2. Adsorption energies

The calculated adsorption energies are compiled in Table II. The first column lists the adsorption energies calculated with respect to the ground state of the clean film, the second column for a fixed magnetic configuration of the clean and the adsorbate-covered films. The striking result is that ad-

TABLE IV. Adsorption properties of CO on γ-Fe/Cu(100) films (coverage $\theta=0.5$ ML). Adsorption energy E_{ad} (in eV/molecule), buckling of the top Fe layer Δz_{Fe} (in Å), height of the C atom above the top layer z_{C} (in Å), bond length of the molecule $d_{\mathrm{C\text{-}O}}$ (in Å), adsorption-induced change in the average film thickness Δd (in % of the interlayer spacing of the substrate), and adsorption-induced change in the film magnetization $\Delta\mu$ (in μ_B).

Magnetic configuration	Adsorption site	E_{ad}[a]	Δz_{Fe}	z_{C}	$d_{\mathrm{C—O}}$	Δd	$\Delta\mu$
uudd	bridge	−1.534	0.01	1.47	1.19	−1.5	0.84
	hollow	−1.480	0.00	1.04	1.21	−1.9	0.87
	top	−1.336	0.09	1.73	1.17	−3.1	0.92
uuuu	bridge	−1.539	0.05	1.49	1.19	0.8	−0.73
	hollow	−1.471	0.00	1.03	1.22	0.4	−0.63
	top	−1.270	0.17	1.68	1.17	−7.3	−1.42
uuud	bridge	−1.888	0.02	1.46	1.19	−3.1	0.90
	hollow	−1.605	0.00	1.10	1.21	+1.1	0.46
	top	−1.746	0.06	1.75	1.17	−4.2	0.76

[a]Calculated with respect to the same magnetic configuration of the clean film.

sorption on a film with a mixed magnetic (uuud) configuration produces a much larger adsorption energy than on either a bilayer AFM or a FM film—the energy gain is even sufficient to exceed the magnetic energy difference calculated for the clean films such that at a monolayer coverage of CO the uuud configuration is lower in energy than the uudd state by about 0.1 eV/molecule. Besides, the change of the magnetic configuration induced by the adsorption gives rise to a large increase of the overall magnetization of the film and to a reduction of the film thickness.

With about 1 eV/molecule, the calculated adsorption energies are quite modest. This is a consequence of the strong lateral repulsions between the adsorbed molecules. For a free-standing monolayer of CO molecules oriented perpendicular to the layer and with the lattice constant of the Cu(100) substrate, we calculate a repulsive energy of 0.68 eV/molecule.

3. Properties of the adsorbate

The properties of the adsorbed CO molecule collected in Table II are determined mostly by the adsorption geometry and much less by the magnetic configuration of the adsorbate. The height of the C atom above the surface varies between about $z_{\mathrm{C}}\approx 0.95$ Å (hollow), $z_{\mathrm{C}}\approx 1.50$ Å (bridge), and z_{C} between 1.50 to 1.80 Å (on top). The C−O bond length is stretched slightly compared to the molecule in the gas phase ($d_{\mathrm{C\text{-}O}}=1.144$ Å), the elongation of the molecular bond increasing with the surface coordination: $d_{\mathrm{C\text{-}O}}=1.16$ Å, 1.17 Å and 1.20 Å for top, bridge, and hollow, independent of the magnetic configuration of the substrate. The interaction with the magnetic film induces also a weak spin polarization of the adsorbate. The magnetic moment on the C atom is always antiparallel to the Fe moment in the surface layer and roughly proportional to its magnitude, i.e., the largest induced moments of about 0.04 to $0.05\mu_B$ are found for uuuu and uudd films and the C atom in bridge or hollow positions; for uuud films the induced moment is only $0.02\mu_B$ in the stable bridge position. Induced moments on the O atoms are always significantly smaller.

4. Electronic structure of the adsorbate-substrate complex

To elucidate the physical mechanisms determining the adsorbate-substrate bonding and the resulting changes in the structure and magnetism of the substrate, we have examined the adsorbate-induced changes in the electronic spectra and in the spatial distribution of charge and spin densities at the surface. Quite generally we expect donation of electrons from the d orbitals of the substrate to the π orbitals of the adsorbed CO molecule, combined with back donation from the adsorbate into covalent adsorbate-substrate bonds. The highest occupied molecular orbitals of the free CO molecule are the 4σ, 1π, and 5σ states; the lowest unoccupied molecular eigenstate is the $2\pi^*$ state. Upon adsorption, the energies of the molecular eigenstates are lowered with respect to the Fermi energy such that the 1π and 5σ states lie just below the bottom of the Fe d band. The $2\pi^*$ state overlaps with the upper part of the d band and becomes partially occupied. Due to the exchange splitting, the interaction with minority electrons is stronger than with majority electrons. The details of the charge flow will depend on the adsorption geometry and on the magnetic structure of the substrate, since different orbitals will be involved in the process. Figure 1 shows isosurfaces of difference-electron densities for the CO molecule adsorbed in the bridge position, Fig. 2 for hollow adsorption on a film with a magnetic configuration uuud. The difference-electron densities are defined as

$$\Delta\rho=\rho(\mathrm{CO+Fe/Cu})-\rho(\mathrm{CO})-\rho(\mathrm{Fe/Cu}),$$

where $\rho(\mathrm{CO+Fe/Cu})$ stands for the electron density of the adsorbate-substrate complex, $\rho(\mathrm{CO})$ the electron density of gas phase CO, and $\rho(\mathrm{Fe/Cu})$ for the charge density of the clean film, all atoms being placed into the positions they occupy in the relaxed adsorbate-covered film.

For bridge-site adsorption, mainly the Fe t_{2g} (d_{yz} and d_{xy}) orbitals are depleted, but also the bonding σ states of

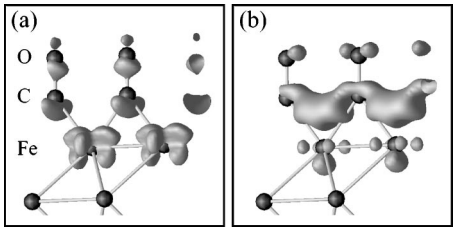

FIG. 1. Isosurfaces of the difference-electron densities for CO adsorbed in a bridge position on a 4-ML Fe/Cu(100) film with the magnetic configuration uuud. Panel (a) shows regions of decreased electron densities, (b) regions of increased charge densities. See text.

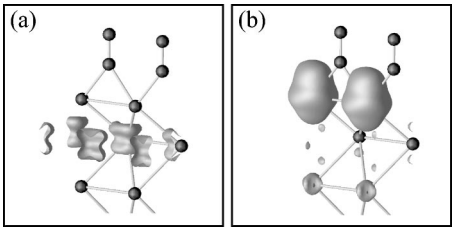

FIG. 3. Isosurfaces of the difference-magnetization densities for CO adsorbed in a bridge position on a 4-ML Fe/Cu(100) film with the magnetic configuration uuud. Panel (a) shows regions of decreased magnetization densities, (b) regions of enhanced magnetization densities. See text.

the molecule [see Fig. 1(a)]. Charge flows into the adsorbate-substrate bonds and into π states of the adsorbate [see Fig. 1(b)]. The fact that back donation from the adsorbate to the substrate is very limited explains the strong adsorbate-induced inward relaxation of the top layer: the $d \rightarrow \pi$ donation reduces the occupation of antibonding d states, and since no compensating back donation takes place the Fe-Fe bond strength is increased.

For adsorption in the hollow positions the pattern shown by the difference-electron densities is quite different as visible in Fig. 2: the depletion of the Fe t_{2g} orbitals affects mostly the in-plane d_{xy} state and note also a stronger depletion of the bonding σ states of the adsorbate. Charge flows into the Fe$-$CO adsorbate-substrate bonds, but surprisingly also into the region of the back bonds between surface and subsurface atoms, leading to an increased occupation of antibonding d states which has not been observed for bridge-site occupation. This explains the surprising differences in the relaxation behavior (see Table I) predicted for these two different configurations. For a given adsorbate geometry, the charge redistribution is almost independent of the magnetic structure of the substrate—for bridge-site adsorption on an uudd film we obtain almost exactly the same picture as for uuud configuration illustrated by Fig. 1. However, the charge redistribution affects electrons of different spin.

To see the influence of the magnetic configuration of the substrate, we have to analyze the adsorbate-induced changes in the spin or magnetization densities. This is illustrated in Figs. 3 and 4 showing isosurfaces of the difference-magnetization densities $\Delta\mu$ (defined in the same way as the difference-electron densities $\Delta\rho$) for bridge-adsorbed CO on uuud and uudd films. For the uuud film, the positive $\Delta\mu$ values around the Fe atoms in the top layer reflect the reduction of the negative surface moments, the negative $\Delta\mu$ values the decrease of the positive moments in the subsurface layer. In contrast to the changes in the electron densities occurring largely in the bonding regions, the changes in the magnetization densities are localized at the atomic sites. The absence of significant charge-density changes in the second and third layers, together with changes in the magnetization densities at these sites, shows that a substantial fraction of the adsorbate-induced changes in the magnetic moments arises from intra-atomic redistributions between majority- and minority-spin states. For bridge-adsorbed CO on a film with the antiferromagnetic bilayer configuration uudd (see Fig. 4) $\Delta\mu$ is positive around all Fe atoms in the three top layers (i.e., reduction of the negative moments in the surface bilayer and a slight enhancement of the positive moment in the third layer, see Table I). Whereas the change in the magnetization density at the top sites is rather delocalized, it is strictly localized and largely intra-atomic on the subsurface sites. In this case the positive $\Delta\mu$ surface extends to the Fe $-$CO bonding region and to the π^* states localized on both the C and O atoms, reflecting a spin polarization of the covalent bond and a small magnetic polarization of the CO molecule induced by covalent interactions.

To complete the analysis and to get a deeper insight into the correlation between adsorption and surface magnetism, we have analyzed the local densities of states (DOS). Figure 5 displays the result for bridge adsorption on an uuud film, i.e., the stable configuration at a full CO coverage, Fig. 6 shows the same information for the less favorable hollow

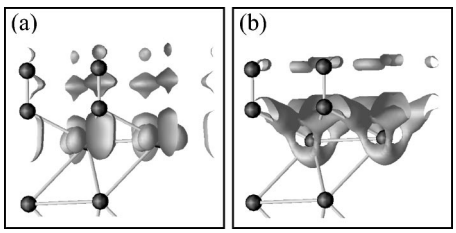

FIG. 2. Isosurfaces of the difference-electron densities for CO adsorbed in a hollow position on a 4-ML Fe/Cu(100) film with the magnetic configuration uuud. Panel (a) shows regions of reduced electron densities, (b) regions of increased charge densities. See text.

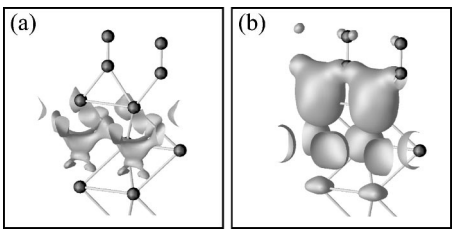

FIG. 4. Isosurfaces of the difference-magnetization densities for CO adsorbed in a bridge position on a 4-ML Fe/Cu(100) film with the magnetic configuration uudd. Panel (a) shows regions of decreased magnetization densities, (b) regions of enhanced magnetization densities. See text.

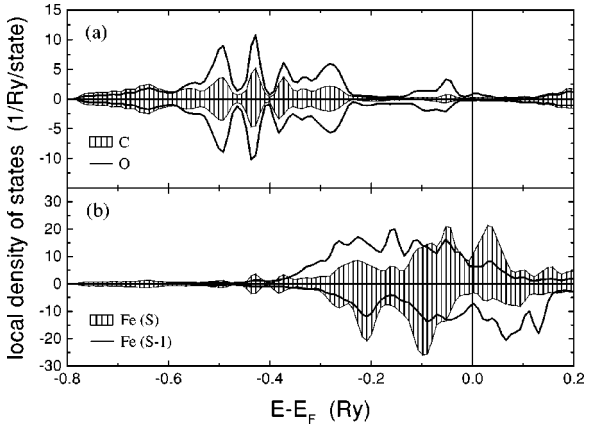

FIG. 5. Spin-polarized local electronic densities of states of a CO-covered Fe/Cu(100) film in the magnetic configuration uuud and CO in the bridge positions. The hatched areas denote the densities of state of C or surface Fe atoms, the solid lines those of O or subsurface Fe atoms.

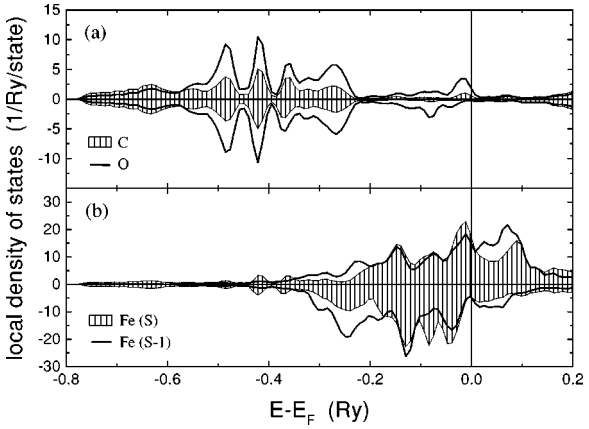

FIG. 7. Spin-polarized local electronic densities of states of a CO-covered Fe/Cu(100) film in the magnetic configuration uudd and CO in the bridge positions. The hatched areas denote the densities of state of C or surface Fe atoms, the solid lines those of O or subsurface Fe atoms. Compare with Fig. 5.

site. The local DOS on the C and O atoms show two characteristic peaks at binding energies of about 5.4 eV and 6.8 eV arising from the 5σ and 1π states and a broad distribution of states at lower binding energies overlapping with the *d* band of the substrate, arising from a partial occupation of 2π states. While the position of the former two peaks is almost the same for both bridge and hollow adsorption, the DOS attributed to the $2\pi^*$ states show a pronounced dependence on the adsorption site. Likewise, we find that the different adsorption geometries lead to significant differences in the local DOS of the top layer of the substrate. For CO in the stable bridge position, the Fermi level falls into pronounced DOS minima for both the majority (d) and minority (u) bands whereas for CO in the fourfold hollow, the spin-up DOS reveal a sharp maximum precisely at the Fermi level leading to an enlarged band energy. For the subsurface layer the differences in the local DOS are less pronounced, but here again the band structure clearly favors adsorption in the bridge site. The adsorption geometry also influences the electron donation into the 2π states: in the hollow position where the adsorbed molecule comes much closer to the surface we find a higher occupation of the antibonding state, explaining in turn the more pronounced stretching of the C $-$O bond.

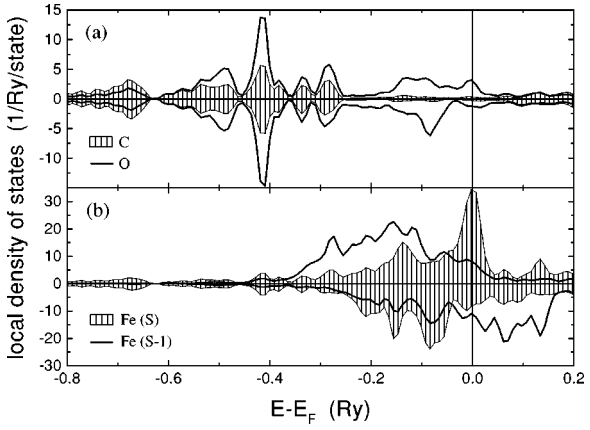

FIG. 6. Spin-polarized local electronic densities of states of a CO-covered Fe/Cu(100) film in the magnetic configuration uuud and CO in the hollow positions. The hatched areas denote the densities of state of C or surface Fe atoms, the solid lines those of O or subsurface Fe atoms.

If we compare the DOS for the uuud configuration stabilized by the CO overlayer with that of the less stable uudd configuration (see Figs. 5 and 7), we find that the electronic states of the adsorbate are hardly affected by the change in the magnetic structure of the substrate (except for marginal changes in the local DOS of carbon near E_F), but substantial differences exist in the DOS of the top layers of the substrate. The reduction of the magnetic moment and of the exchange splitting is here relatively modest for the top layer (from $2.82\mu_B$ to $2.18\mu_B$, see Table I), and at the slightly increased filling of the minority band the Fermi level falls close to a DOS maximum. For the subsurface layer, the reduction of the magnetic moment is more pronounced, but we note a similarly unfavorable form of the minority DOS at the Fermi level. A similar destabilizing effect is found for bridge-adsorbed CO on a ferromagnetic film. Radnik *et al.*[28] have probed CO adsorption on γ-Fe films grown on Cu(100) and on polycrystalline α-Fe using ultraviolet photoemission spectroscopy and reported significant differences in the relative intensities of the emission peaks due to 4σ, 5σ, and 1π states of CO on both surfaces, which was attributed to differences in the photoionization cross sections for upright and ''lying-down'' CO molecules. These differences cannot be probed by the present calculations, but the calculated positions of the CO emission peaks are in reasonable agreement with experiment.

B. Fe/Cu(100) covered by a half a monolayer of CO

For a 0.5 ML coverage, the calculations have been carried out for (2×1) surface cells. This choice leads to an arrangement of the adsorbed CO molecules in straight rows and does not maximize the intermolecular distance in the adsor-

bate layer. At this coverage, a $(\sqrt{2}\times\sqrt{2})$ superstructure is probably energetically more favorable, however, for a $(\sqrt{2}\times\sqrt{2})$ superstructure and CO in hollow or bridge positions, all Fe sites in the top layer would be equivalent, whereas for the (2×1) structure this holds only for hollow adsorption. Hence our choice of the adsorption geometry allows to distinguish between substrate atoms bonded or nonbonded to the adsorbate without increasing the size of the supercell.

1. Structure, magnetism, and energetics

Table III summarizes the results for the structural and magnetic properties of a film covered by half a monolayer of CO. Full details of the adsorbate-induced reconstruction of the film are given only for the stable adsorption site at each magnetic configuration. The calculations have been performed using a (2×1) cell, hence for CO in an on-top or bridge position, the two iron atoms in the surface cell are inequivalent, whereas for an adsorption in the fourfold hollow all atoms are equivalent. Accordingly, in the former case we expect a certain degree of buckling, whereas in the latter case the surface remains flat. At this lower coverage, adsorption does not lead to a change of the stable magnetic configuration of the substrate—the uudd bilayer phase remains energetically preferred, although the magnetic energy difference relative to the mixed uuud phase is strongly reduced, from 442 meV/cell for the clean film to 89 meV/cell after CO adsorption. The energy difference relative to the ferromagnetic uuuu phase remains essentially unchanged. Independent of the magnetic state of the substrate, adsorption in a bridge site is always energetically favored, although for the uudd and uuuu phases the difference in the adsorption energy for bridge and hollow is quite small. For all possible adsorption modes the magnetic moments of the surface atoms directly bonded to the adsorbate are strongly reduced while the moments at the free sites are even slightly enhanced. For the antiferromagnetic uudd configuration this leads to a reversal of the sign of the total magnetization from a small negative to a small positive value, for the mixed uuud configuration the positive magnetization is increased, and for the ferromagnetic configuration the total magnetization is reduced. In the case of a film in the stable uudd state, CO adsorption reduces the surface moment on these Fe atoms to about half its value on a clean film whereas the moments on the other surface sites remain essentially unchanged. Hence a partial coverage leads to the formation of a magnetic pattern on the surface. This effect is even stronger for a film in the uuud configuration, where the difference in the magnetic moments of neighboring surface atoms can amount to $2\mu_B$ and for CO in a top site on a ferromagnetic film with the difference in the magnetic moments, even $2.4\mu_B$.

The adsorbate-induced changes in the film geometry are relatively modest. For bridge-adsorbed CO on a uudd film a slight contraction is predicted. The change in the interlayer distances is larger between the second and third than between the top layers, because at the surface the contraction due to the reduced moments is partly compensated by an adsorbate-induced outward relaxation. Surface buckling remains very modest. Larger adsorption-induced restructuring is predicted only for on-top adsorption which is, however, energetically disfavored.

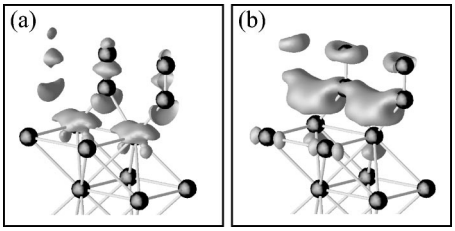

FIG. 8. Isosurfaces of the difference-electron densities for CO (0.5-ML coverage) adsorbed in a bridge position on a 4-ML Fe/Cu(100) film with the magnetic configuration uudd. Panel (a) shows regions of reduced electron densities, (b) regions of increased charge densities. See text.

2. Properties of the adsorbate

The calculated properties of the adsorbate are summarized in Table IV. Compared to the full monolayer we note a bit more pronounced stretching of the C−O bond length, in accordance with the larger adsorption energy. In the stable bridge position, the distance of the C atom from the surface is about the same as that at a full monolayer coverage. Compared to full monolayer coverage, the adsorption energy for CO in bridge sites increases by 0.46 eV/molecule for a film in the stable antiferromagnetic bilayer configuration uudd, and even by 0.71 eV/molecule for a film in the less stable configuration uuud. While a difference of about 0.4 eV/molecule can be attributed to the decrease of the lateral repulsions between the adsorbed molecules, the extra difference found for adsorption on the uuud film is due to the fact that in this case the very strong local demagnetization reduces the magnetic frustration between surface and subsurface layers.

3. Electronic structure of the adsorbate-substrate complex

For bridge-adsorbed CO on a bilayer antiferromagnetic film the pattern of adsorption-induced charge flows is qualitatively similar than for full monolayer coverage, but we note a somewhat increased depletion of the bonding σ states and an increased population of the antibonding $2\pi^*$ states of the adsorbed molecule, in line with a larger stretching of the C−O bond. At the free Fe sites, the occupation of p bands increases a bit. In the difference-magnetization densities (see Figs. 8 and 9) we find locally the same changes as on the fully CO-covered surface at those sites forming covalent bonds to the CO molecule. In addition we find strictly localized changes in the magnetization densities at the free-surface sites and at the Fe sites in the deeper layers, arising from interatomic redistributions between spin-up and spin-down states. These spin redistributions are associated with local changes in the exchange splitting between spin-up and spin-down bands, but the local variations in the DOS will not be discussed in further detail here.

C. Vibrational spectroscopy of the adsorbate

Infrared reflection absorption spectroscopy (IRRAS) of CO adsorbed on γ-Fe/Cu(100) films of varying thicknesses

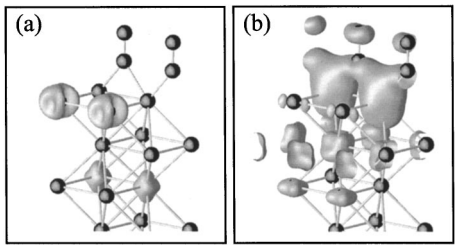

FIG. 9. Isosurfaces of the difference-magnetization densities for CO (0.5-ML coverage) adsorbed in a bridge position on a 4-ML Fe/Cu(100) film with the magnetic configuration uudd. Panel (a) shows regions of reduced magnetization densities, (b) regions of increased magnetization densities. See text.

has been reported by Tanabe *et al.*[29] For a 2-ML film at low exposure (0.14 L) a C−O stretch band at 1930 cm^{-1}, with a weak shoulder at the high-frequency side, has been reported. At increased exposure (0.26 L) the main IR band is intensified and shifted to 1954 cm^{-1}, while the shoulder at 2010 cm^{-1} becomes also more pronounced. A further increase of the CO partial pressure leads to a reversal of the intensities of the low- and high-frequency structures in the IRRAS band, until at saturation (1.1 L) only a rather sharp cusp at about 2030 cm^{-1} survives. The low-frequency feature has been attributed to bridge-adsorbed CO and that at higher frequencies to on-top-adsorbed CO. This assignment is based on IRRAS on metal-carbonyl complexes where the C−O stretch band at $\geqslant$2000 cm^{-1} has been found to be associated with CO bonded to a single metal atom, whereas it is positioned at 1850 to 2000 cm^{-1} for bridge-bonded CO and below 1850 cm^{-1} for CO in threefold coordination. Electron-energy-loss spectroscopy for CO adsorbed on bcc Fe surfaces identified three C−O stretch band at frequencies of 1325 to 1575 cm^{-1}, 1750 to 1860 cm^{-1}, and 1940 to 2015 cm^{-1} attributed to adsorption in deep and shallow hollows and on-top sites, respectively. For 6-ML Fe/Cu(100) a similar picture with a low-frequency band at 1915 to 1934 cm^{-1} and a high-frequency band at 2000 to 2038 cm^{-1} was reported. Only the high-frequency feature survives at saturation, but at all frequencies both bands largely overlap. Evidently the assignment of the high-frequency band with on-top-adsorbed CO is at variance with our prediction that the on-top site is always energetically disfavored with respect to both bridge and hollow sites. Surprisingly, the CO stretch frequency measured at saturation does not change when the thickness of the film exceeds 10 to 12 ML and the structure reverts from fcc to bcc—this would suggest that the surfaces of bulk bcc Fe and bcc Fe/Cu(100) are quite different even in this regime. Our results for the C−O and Fe−C stretch frequencies calculated for 1-ML CO on a film with the mixed magnetic uuud configuration and for 0.5-ML CO on a bilayer antiferromagnetic film are compiled in Table V. At half monolayer coverage, the frequencies calculated for hollow, bridge, and top adsorption agree reasonably well with the assignment based on the measured IRRAS bands for metal carbonyls and scale with the calculated elongation of the C−O bond. The C−O stretching frequency of 1877 cm^{-1} calculated for bridge-adsorbed CO agrees well with the experimental frequencies measured at low exposure, remembering that for gas phase CO the calculated frequency of 2114 cm^{-1} is also slightly lower than the experimentally measured one, 2170 cm^{-1}. At full coverage, we predict a pronounced blueshift of the CO stretching frequency to 2004 cm^{-1} for bridge-adsorbed CO. At this high coverage, the stretching frequency for on-top-adsorbed CO is already very close to that of the gas phase molecule. The blueshift of the C−O stretching frequency is accompanied by a softening of the Fe−C stretching frequency, in agreement with the weaker adsorbate-substrate interaction. Our results offer an alternative interpretation of the experimental findings of Tanabe *et al.*[29] our stretching frequency of 2004 cm^{-1} for bridge-adsorbed CO at full coverage is in reasonable agreement with their result measured at saturation. Hence the observed changes of the IRRAS spectra with CO exposure reflect a change in the strength of the adsorbate-substrate bonding rather than a change in the adsorption geometry. This is supported by the observation that at any coverage, the measured IRRAS band shows a broad, rather asymmetric peak and not a two-peak structure. Therefore the experimental observations are certainly compatible with a gradual shift of the C−O stretching frequency with coverage. The observed asymmetry of the peaks could arise from the coexistence of domains with different CO coverages.

TABLE V. C−O and C−Fe stretching frequencies (in cm^{-1}) for CO adsorbed in high-symmetry positions on a 4-ML Fe/Cu(100) film at different coverages. At each coverage, the calculation has been performed for the respective magnetic ground state (uudd at 0.5-ML CO, uuud at 1-ML CO).

Coverage	Magnetic configuration	Adsorption site	$\omega_{C\text{-}O}$	$\omega_{C\text{-}Fe}$
0.5 ML	uudd	bridge	1877	399
		hollow	1661	266
		top	1971	420
1.0 ML	uuud	bridge	2004	356
		hollow	1760	254
		top	2103	402

IV. DISCUSSION AND CONCLUSIONS

We have presented detailed first-principles calculations of the adsorption of CO on ultrathin γ-Fe films grown on a Cu(100) substrate. In accordance with previous experimental observations we find that CO is adsorbed in molecular form and in an upright position. Independent of the coverage and of the magnetic configuration we find that bridge adsorption is energetically preferred over hollow or on-top adsorption. This contradicts the current interpretation of the IRRAS experiments assuming a change from bridge to on-top adsorption as the coverage of the film approaches saturation. However, our calculations show a pronounced increase of the C−O stretching frequency for bridge-adsorbed CO as the coverage is increased from 0.5 to 1 ML. The shift of the C−O

frequency is even in quantitative agreement with experiment. Hence our results predicting bridge adsorption only are in agreement with the experimental observation. Our calculations also predict measurable differences for the Fe−C stretching frequencies for bridge and on-top adsorption—an experimental study of these low-frequency modes could clarify the question of the adsorption geometry.

The most important result of our study is the strong influence of the adsorbate on the magnetic properties of the substrate. Quite generally we find a substantial reduction of the magnetic moments at the surface of the film, the details of the demagnetization depending strongly on the magnetic configuration of the substrate, the adsorption geometry, and the coverage. For the 4-ML Fe film considered in the presented work, the calculated magnetic ground state is bilayer antiferromagnetic, with only a modest magnetic energy difference to the ferromagnetic phase. At a complete monolayer coverage, however, the magnetic ground state switches to a uuud sequence, i.e., a largely demagnetized surface is coupled antiferromagnetically to a ferromagnetic rest. In terms of the total magnetization, a monolayer of adsorbed CO induces a change from an almost compensated antiferromagnet to a large total magnetic moment of about $1.53\mu_B$/Fe atom. The change of the magnetic ground state is accompanied by an ample inward relaxation of the top layer caused by the antiferromagnetic interlayer coupling.

At a coverage of half a monolayer, the magnetic ground state remains the same as for the clean film but we find a strong demagnetization of the Fe atoms directly bonded to the adsorbate, while the magnetism of the free Fe sites is even slightly increased. The origin of the demagnetization can be traced back to the back donation of electrons into minority bands of the substrate. It is interesting to point out that while the demagnetization is strictly localized in the lateral directions, it can extend to the deeper layers of the substrate. This is particularly evident for bridge-site adsorption at full coverage for a uudd film. Here the reduction of moments is even stronger on the subsurface Fe atoms positioned directly below the adsorbate. Mostly via magnetovolume effects, this demagnetization also leads to a restructuring (change of relaxation pattern, buckling) of the substrate. This effect is rather distinct at full coverage.

The fact that molecular adsorption can be used to create a magnetically structured surface is an extremely interesting observation. So far, to the best of our knowledge, no attempts have been made to optimize the superstructure of the adsorbate-substrate complex. For nonmagnetic substrates [e.g., CO on Rh(100)] previous studies[43] have identified complex superstructures with mixed on-top and bridge sites representing a coincidence lattice determined essentially by the interplay of the square lattice of the substrate and a hexagonal lattice minimizing the lateral repulsions between the adsorbed molecules. In the present case the magnetic interactions in the surface layer adds a new dimension to the problem. In this sense work like that, presented here, together with similar studies on adsorption-induced changes of magnetic surfaces[2,44] open a line of research.

ACKNOWLEDGMENTS

One of the authors (D.S.) has profited from numerous conversations with A. Eichler. This work has been supported by the Austrian Ministry for Science and Transport within the project ''Magnetism on the Nanometer Scale'' and through the Center for Computational Materials Science.

[1] P.W. Selwood, *Chemisorption and Magnetism* (Academic Press, New York, 1975).
[2] Q. Ge, S.J. Jenkins, and D.A. King, Chem. Phys. Lett. **327**, 125 (2000).
[3] J. Thomassen, F. May, B. Feldmann, M. Wuttig, and H. Ibach, Phys. Rev. Lett. **69**, 3831 (1992).
[4] Th. Detzel, M. Vonbank, M. Donath, and V. Dose, J. Magn. Magn. Mater. **147**, L1 (1995).
[5] W.A.A. Macedo and W. Keune, Phys. Rev. Lett. **61**, 475 (1988).
[6] H. Magnan, D. Chandresis, B. Vilette, O. Heckmann, and J. Lecante, Phys. Rev. Lett. **67**, 859 (1991).
[7] S. Müller, P. Bayer, C. Reischl, K. Heinz, B. Feldmann, H. Zillgen, and M. Wuttig, Phys. Rev. Lett. **74**, 765 (1995).
[8] K. Heinz, S. Müller, and P. Bayer, Surf. Sci. **352-4**, 942 (1996).
[9] R.D. Ellerbrock, A. Fuest, A. Schatz, W. Keune, and R.A. Brand, Phys. Rev. Lett. **74**, 3053 (1995).
[10] D.J. Keavney, D.F. Storm, J.W. Freeland, I.L. Grigorov, and C. Walker, Phys. Rev. Lett. **74**, 4531 (1995).
[11] M. Straub, R. Vollmer, and J. Kirschner, Phys. Rev. Lett. **77**, 743 (1996).
[12] N. Memmel and Th. Detzel, Surf. Sci. **307-309**, 490 (1994).
[13] M. Zharnikov, A. Dittschar, W. Kuch, C.M. Schneider, and J. Kirschner, Phys. Rev. Lett. **76**, 4620 (1996).
[14] W. Platow, M. Ferle, and K. Baberschke, Europhys. Lett. **43**, 713 (1998).
[15] A. Berger, B. Feldmann, H. Zillgen, and M. Wuttig, J. Magn. Magn. Mater. **183**, 35 (1998).
[16] H. Zillgen, B. Feldmann, and M. Wuttig, Surf. Sci. **321**, 32 (1994).
[17] C.L. Fu and A.J. Freeman, Phys. Rev. B **35**, 925 (1987).
[18] T. Kraft, P.M. Marcus, and M. Scheffler, Phys. Rev. B **49**, 11 511 (1994).
[19] R. Lorenz and J. Hafner, Thin Solid Films **281**, 492 (1996); Phys. Rev. B **54**, 15 937 (1996).
[20] T. Asada and S. Blügel, Phys. Rev. Lett. **79**, 507 (1997).
[21] E.G. Moroni, J. Hafner, and G. Kresse, J. Phys.: Condens. Matter **11**, L35 (1999); J. Magn. Magn. Mater. **198-199**, 551 (1999).
[22] D. Spišák and J. Hafner, Phys. Rev. B **61**, 16 129 (2000).
[23] R. Vollmer and J. Kirschner, Phys. Rev. B **61**, 4146 (2000).
[24] G.J. Mankey, M.T. Kief, F. Huang, and R.F. Willis, J. Vac. Sci. Technol. A **11**, 2034 (1993).
[25] G. Ertl, in *Catalysis*, edited by J.R. Anderson and M. Boudart (Springer, Berlin, 1983), Vol. 4, p. 209.
[26] T.J. Vink, O.L.J. Gijzeman, and J.W. Geus, Surf. Sci. **150**, 14 (1985).
[27] H. den Daas, E.H. Voogt, O.L.J. Gijzeman, and J.W. Geus, Surf. Sci. **306**, 1 (1994).

[28] J. Radnik, E. Chopovskaya, M. Grüne, and K. Wandelt, Surf. Sci. **352-354**, 268 (1996).
[29] T. Tanabe, Y. Suzuki, T. Wadayama, and A. Hatta, Surf. Sci. **427-428**, 414 (1999); T. Tanabe, T. Shibahara, R. Buckmaster, T. Ishibashi, T. Wadayama, and A. Hatta, *ibid.* **466**, 1 (2000).
[30] A. Kirilyuk, J. Giergiel, J. Shen, M. Straub, and J. Kirschner, Phys. Rev. B **54**, 1050 (1996).
[31] G. Kresse and J. Hafner, Phys. Rev. B **48**, 13 115 (1993).
[32] G. Kresse and J. Furthmüller, Phys. Rev. B **54**, 11 169 (1996); Comput. Mater. Sci. **6**, 15 (1996).
[33] E.G. Moroni, G. Kresse, J. Hafner, and J. Furthmüller, Phys. Rev. B **56**, 15 629 (1997).
[34] G. Kresse and D. Joubert, Phys. Rev. B **59**, 1758 (1999).
[35] P. Blöchl, Phys. Rev. B **50**, 17 953 (1994).
[36] D. Vanderbilt, Phys. Rev. B **41**, 7892 (1990).
[37] G. Kresse and J. Hafner, J. Phys.: Condens. Matter **6**, 8245 (1994).
[38] J. Perdew and A. Zunger, Phys. Rev. B **23**, 5048 (1981).
[39] S.H. Vosko, L. Wilk, and M. Nusair, Can. J. Phys. **58**, 1200 (1980).
[40] J.P. Perdew, Phys. Rev. B **33**, 8822 (1986).
[41] J.P. Perdew, J.A. Chevary, S.H. Vosko, K.A. Jackson, M.R. Pedersen, D.J. Singh, and C. Fiolhais, Phys. Rev. B **46**, 6671 (1992).
[42] H.J. Monkhorst and J.D. Pack, Phys. Rev. B **13**, 5188 (1976).
[43] A. Eichler and J. Hafner, J. Chem. Phys. **109**, 5585 (1998).
[44] A. Eichler and J. Hafner, Phys. Rev. B **62**, 5163 (2000).